# Numerical Simulation of Reactive Extrusion Processes of PA6

**Lili Wu,[1] Yuxi Jia,[1,2] Sheng Sun,[1] Guofang Zhang,[1] Guoqun Zhao,[1] Lijia An[2]**

[1]*School of Materials Science and Engineering, Shandong University, Jinan 250061, People's Republic of China*
[2]*State Key Laboratory of Polymer Physics and Chemistry, Changchun Institute of Applied Chemistry, Chinese Academy of Sciences, Changchun 130022, People's Republic of China*

Received 13 January 2006; accepted 15 May 2006
DOI 10.1002/app.24815
Published online in Wiley InterScience (www.interscience.wiley.com).

**ABSTRACT:** To analyze the complicated relationships among the variables during the reactive extrusion process of polyamide 6 (PA6), and then control the chemical reaction and the material structures, the process of continuous polymerization of caprolactam into PA6 in a closely intermeshing co-rotating twin screw extruder was simulated by means of the finite volume method, and the influences of three key processing parameters on the reactive extrusion process were discussed. The simulated results of an example were in good agreement with the experimental results. © 2006 Wiley Periodicals, Inc. J Appl Polym Sci 103: 2331–2336, 2007

**Key words:** reactive extrusion; anionic polymerization; polyamide 6; numerical simulation

## INTRODUCTION

The reactive extrusion process is a new kind of technology in the field of polymer processing. Using twin screw extruders as reactors, the reactive extrusion for polymerization can realize an integrated process of the chemical reaction and the continuous extrusion. The investigations into the polymerization of polyamide 6 (PA6) in extruders can date back to 1968; it was Illing who reported the method of the anionic polymerization of caprolactam into PA6 in twin screw extruders.[1,2] Since the 1980s, Menges, Michaeli, and Berghaus and their colleagues at the University of Aachen and the IKV Company,[3–6] as well as Hornsby and Tung at the University of Brunel[7] and White and Kye at the University of Akron,[8–11] all applied themselves to the research of this process.

Most of the investigations into the reactive extrusion process of PA6 were concentrated on the experiments. There are complex interactions among such phenomena as fluid flow, heat transfer and chemical reaction during the reactive extrusion process, which cause the theoretical research to be very difficult.[1–11] The existing theoretical investigations have been mainly confined to one-dimensional (1D) models and have generally simplified the complicated relationships among fluid flow, chemical reaction, material structures, physicochemical properties, and heat transfer.

Therefore, establishing an equivalent reactor model, adopting a semi-implicit iterative algorithm to deal with the complicated relationships among the various variables, and numerically simulating the reactive extrusion process of PA6 have the important scientific significance and the engineering value.

In the present study, on the basis of Michaeli's experimental research,[4] the numerical simulation of the reactive extrusion process for the polymerization of caprolactam in co-rotating twin screw extruders is developed via the finite volume method, and the evolution of the key variables is analyzed numerically. Then the influences of several processing parameters on reactive extrusion processes are discussed. The simulated results are compared with Michaeli's calculated results and experimental results.

## METHODS AND STEPS OF NUMERICAL SIMULATION

### Construction of the equivalent reactor model

The experimental research on the polymerization of PA6 was carried out in co-rotating twin screw extruders by Michaeli.[4] The mathematical model of co-rotating twin screw extruders developed in most of the investigations was a 1D groove model. Nevertheless, to show the distribution characteristics of various

*Correspondence to:* L. An (ljan@ciac.jl.cn).
Contract grant sponsor: National Natural Science Foundation of China; Contract grant numbers: 50403009; 50573079; 50390096; 50425517; 50340420392.
Contract grant sponsor: Chinese Academy of Sciences; Contract grant number: KJCX2-SW-H07.
Contract grant sponsor: Special Funds for Major State Basic Research Projects; Contract grant number: 2003CB615601.

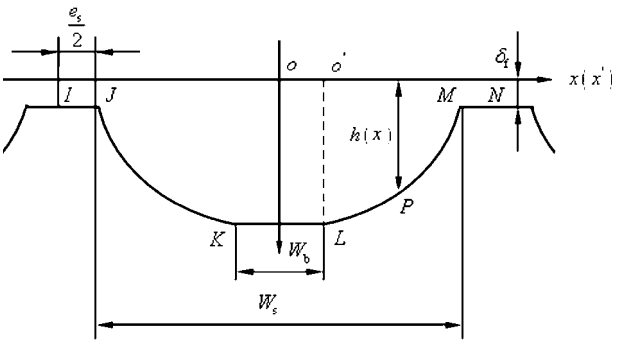


**Figure 1** Cross section of a screw channel.[12]

variables in the cross section of a screw channel, an equivalent model of closely intermeshing co-rotating twin screw extruders is established in this study.

According to the geometry of closely intermeshing co-rotating twin screws,[12] for a double-thread screw, there are three separate parallel fluids in the screw extruder. As in the groove model,[4] the fluid flow space can be unfolded, and the length of the unfolded model, $L_m$,[13] is

$$L_m = \frac{L}{\sin\bar{\phi}}, \tag{1}$$

where $L$ denotes the axial length of the screw, and $\bar{\phi}$ the average helix angle of screws.

Different from the groove model, the unfolded flow space of each fluid is assumed to be axisymmetrical, and the wall of the reactor model is moved along the axial direction of the model at a velocity equivalent to the comprehensive effect of the rotary screws and the static barrel on the fluid flow.

According to the profile of normal screw channels shown in Figure 1,[12] the cross-sectional area of the model is equal to that of normal screw channels, and then the equivalent radius of the model, $R_m$, can be obtained

$$R_m = \left(\frac{2}{\pi}\int_{\frac{W_b}{2}}^{\frac{W_s}{2}}\left\{R_s\left[1+\cos\frac{2\pi\left(x-\frac{W_b}{2}\right)}{T.\cos\bar{\phi}}\right] - \sqrt{C_L^2 - R_s^2\sin^2\frac{2\pi\left(x-\frac{W_b}{2}\right)}{T.\cos\bar{\phi}}} + \delta\right\}dx + \frac{1}{\pi}(2R_s - C_L + \delta)\cdot W_b + \frac{1}{\pi}\delta\cdot W_b\right)^{1/2} \tag{2}$$

where $C_L$ denotes the center line distance of two screws, $R_s$ the radius of the excircle of a screw, $T$ the lead of screws, $\delta$ the single-side gap between screw and barrel, $W_b$ the normal width of the root of a screw channel, and $W_s$ the normal width of the top of a screw channel.

With the parameters listed in Table I,[4,5,12] the equivalent length and radius of the model can be calculated, and then quadrilateral mesh is used to make this model discrete. The number of the nodes in the axial direction of the model is 9000, and the number of the nodes in the radial direction is 60.

## Assumptions of numerical simulation

In our simulation, the following assumptions are made:[12,14,15]

1. The melt leakage in the intermeshing zone and the melt leakage between the barrel and screws are neglected, and the distortion of the fluid from one screw to the other is not taken into account.
2. The extruder is assumed to be fully filled, and the viscous, incompressible, non-isothermal, non-Newtonian fluid flow is also assumed in the extruder.
3. The rate of initiation reaction is much faster than that of the propagation reaction, and initiator molecules all transform to active centers very quickly.
4. The reactant is well stirred, and the distribution of monomer is uniform.
5. All growing chains are formed at the same time and have equal growth probability.
6. No chain transfer or chain termination takes place.
7. Depolymerization is neglected.
8. The distribution of molecular weight of the generated polymer approximately fulfills the Poisson distribution.

## Flowchart and steps of numerical simulation

The variables such as reaction rate, average molecular weight, fluid viscosity, pressure, temperature, and flow velocity interact. Obviously, the variables could not be solved by means of traditional explicit algorithms. Therefore, a semi-implicit iterative algorithm is proposed, which is similar to the self-consistent field method. The flowchart of the numerical simulation is shown in Figure 2.

The specific steps and corresponding formulas are shown as follows.

**TABLE I**
**Main Input Data Correlated to the Twin Screw Extruder**

| Parameters | Numerical values |
|---|---|
| Nominal diameter of screws | 30 mm |
| Centerline distance of screws | 24 mm |
| Slenderness ratio of screws | 29 |
| Number of thread starts | 2 |
| Lead of screws | 28 mm |

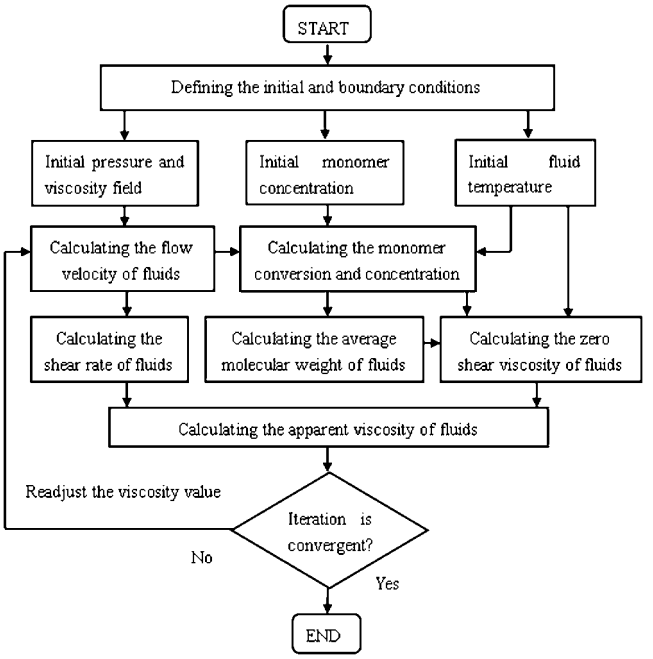


**Figure 2** Flowchart of numerical simulation.

First, the variables are initialized, an initial pressure field $p^*$, and an initial viscosity field $\eta^*$ are defined, and other initial conditions (initial concentration, initial temperature) and boundary conditions are set.

Second, a semi-implicit iterative algorithm is used to solve the conservation equation of momentum, continuity equation, and then the convergent velocity field, pressure field, and shear rate field of fluids are obtained.[16]

The continuity equation is

$$\frac{\partial u_r}{\partial r}+\frac{\partial u_z}{\partial z}+\frac{u_r}{r}=0. \tag{3}$$

The conservation equation of momentum is

$$\frac{\partial u_r}{\partial t}+u_r\frac{\partial u_r}{\partial r}+u_z\frac{\partial u_r}{\partial z}=-\frac{1}{\rho}\frac{\partial p}{\partial r}+\frac{\eta}{\rho}\left(\nabla^2 u_r-\frac{u_r}{r}\right)+F_{br} \tag{4}$$

$$\frac{\partial u_z}{\partial t}+u_r\frac{\partial u_z}{\partial r}+u_z\frac{\partial u_z}{\partial z}=-\frac{1}{\rho}\frac{\partial p}{\partial z}+\frac{\eta}{\rho}\nabla^2 u_z+F_{bz}, \tag{5}$$

where $\rho$ denotes the density of fluids, $p$ the pressure of fluids, $\eta$ the apparent viscosity. $F_{br}$, $F_{bz}$ denote the radial and axial component of the mass force of unit material, respectively, which are ignored in this study.

Third, the fields of monomer conversion, monomer concentration, and average molecular weight are solved sequentially.

The numerical calculation equation of monomer conversion is[4]

$$X(I,J)=\frac{\frac{1-b\cdot X(I-1,J)}{1-X(I-1,J)}\cdot e^{A_p e^{-E_P/RT(I,J)}\Delta t(I,J)(1+b)}-1}{\frac{1-b\cdot X(I-1,J)}{1-X(I-1,J)}\cdot e^{A_p e^{-E_P/RT(I,J)}\Delta t(I,J)(1+b)}+b}, \tag{6}$$

where $X(I, J)$ denotes the monomer conversion in the $I$th time step on the $J$th space point, $X(I–1, J)$ the monomer conversion in the $(I–1)$th time step on the $J$th space point, $T$ the fluid temperature, $\Delta t$ the time step, $A_p$ the frequency factor for chain propagation, $E_p$ the activation energy for chain propagation, $R$ the general gas constant, and $b$ the intensity of autocatalysis.

The numerical calculation equation of monomer concentration is

$$c_m(I,J)=c_{m,0}[1-X(I,J)], \tag{7}$$

where $c_{m,0}$ denotes the initial monomer concentration.

The numerical calculation equation of the equivalent weight-average molecular weight of the fluids, $\overline{M}_{eqw}$, is

$$\overline{M}_{eqw}(I,J)=\frac{M_m c_{m,0}[X(I,J)]^2}{c_i}+M_m[1-X(I,J)], \tag{8}$$

where $M_m$ denotes the molecular weight of monomer, and $c_i$ the concentration of active centers.

Fourth, the apparent viscosity of fluids influenced by monomer conversion, temperature and shear rate is calculated.

The numerical calculation equation of the zero shear viscosity is[17]

$$\eta_0(I,J)=\begin{cases}K_1 e^{\frac{E_\eta}{RT(I,J)}}c(I,J)\overline{M}_w(I,J) & \overline{M}_{eqw}(I,J)\le M_c\\ K_2 e^{\frac{E_\eta}{RT(I,J)}}c^{5.4}(I,J)\overline{M}_w{}^{3.4}(I,J) & \overline{M}_{eqw}(I,J)>M_c\end{cases} \tag{9}$$

where $K_1$ and $K_2$ denote the material constants which are related to temperature, $E_\eta$ the activation energy for fluid flow, $c$ the mass concentration of macromolecular chains, $\overline{M}_w$ the weight-average molecular weight, and $M_c$ the critical molecular weight for entanglement effects in viscosity.

The numerical calculation equation of the apparent viscosity denoted by the Carreau equation is[18]

$$\eta(I,J)=\eta_\infty+[\eta_0(I,J)-\eta_\infty]\cdot\{1+[\lambda\dot{\gamma}(I,J)]^2\}^{\frac{n-1}{2}}, \tag{10}$$

where $\eta_\infty$ denotes the infinite shear viscosity, $\lambda$ the time constant, $\dot{\gamma}$ the shear rate, and $n$ the non-Newtonian index.

Fifth, the results are judged whether they satisfy the condition of convergence. If they are convergent, the

**TABLE II**
**Main Input Data Correlated to the Material and Process**

| Parameters | Numerical values |
|---|---|
| Density of monomer | 1050 kg×m$^{-3}$ |
| Molecular weight of monomer | 113.16 g×mol$^{-1}$ |
| Initial concentration of monomer | 8845.88 mol×m$^{-3}$ |
| Initial concentration of sodium caprolactam | 13.266 mol×m$^{-3}$ |
| Initial concentration of HMDI | 10.08 mol×m$^{-3}$ |
| Frequency factor for chain propagation reaction | 6.3×10$^{5}$ s$^{-1}$ |
| Activation energy for chain propagation reaction | 6.91×10$^{4}$ J×mol$^{-1}$ |
| Activation energy for fluid flow | 40000 J×mol$^{-1}$ |
| The time constant in Carreau equation | 3 s |
| The non-Newtonian index in Carreau equation | 0.5 |
| The infinite shear viscosity in Carreau equation | 100 Pa×s |
| Critical molecular weight for entanglement effects | 19200 g×mol$^{-1}$ |
| Velocity of fluid flow in the entrance of the model | 0.0088 m×s$^{-1}$ |
| Velocity of fluid flow on the wall of the model | 0.0106 m×s$^{-1}$ |

calculation should be ended and the results should be output, whereas the viscosity in the conservation equation of momentum should be readjusted and the computation should be restarted from the second step.

## RESULTS AND DISCUSSION

### Change laws of key variables

According to the experimental condition shown in the paper by Michaeli et al. (their Fig. 23),[4] the main input data correlated to the material and process are listed in Table II.[4,5,19] The evolution of the barrel temperature along the axial direction of the extruder is shown in Figure 3.[4] In the present work, the temperatures of the nodes with the same length of screws are assumed to be identical and equal to the temperature of the corresponding location in the barrel. The inlet velocity is calculated by the feed rate, and the velocity of the wall of the reactor model is determined according to the screw speed as well as the degree of the wall slip. The abscissa $L$ in Figures 3–9 denotes the extruder length, but not the length of the reactor model which is calculated via eq. (1).

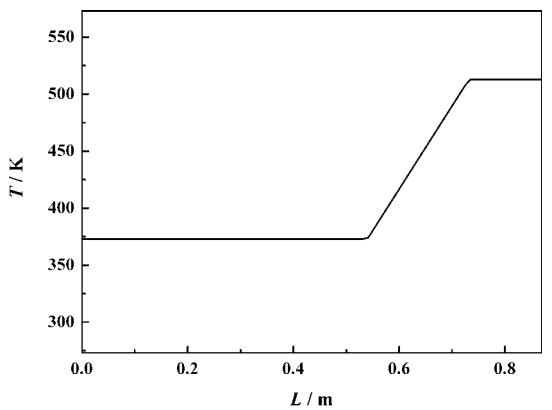


**Figure 3** Evolution of barrel temperature along the axial direction of the extruder.[4]

The evolution of such variables as the monomer conversion, the weight-average molecular weight of the fluid and the apparent viscosity along the axial direction of the extruder are shown in Figures 4–6, respectively (■, 0.0036575 m represents the nodes whose distance to the center line of the reactor model is 0.0036575 m, which is close to the wall of the model; ●, 0.001995 m represents the nodes whose distance to the center line of the model is 0.001995 m; and ▲, 0.0003225 m represents the nodes whose distance to the center line of the model is 0.0003225 m, which is near the center line of the model).

Figures 4–6 show that the increase of the fluid flow length leads to a gradual increase in the monomer conversion, the weight-average molecular weight of the fluid, and the apparent viscosity of the fluid. The reasons are as follows: (1) the monomer conversion is the increasing function of the reaction time and temperature [eq. 6)], and so with the increase of reaction time and temperature, the monomer conversion increases along the axial direction of screws; (2) the influence of the second item in eq. (8) on the weight-average molec-

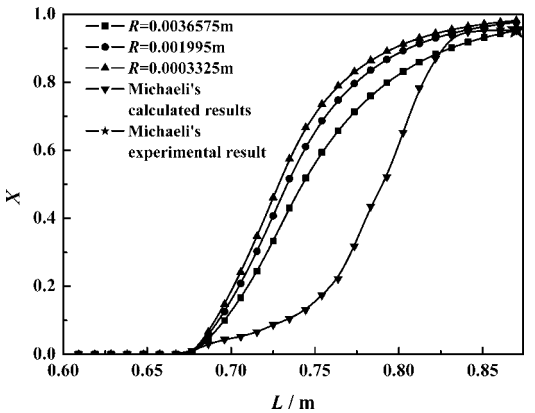


**Figure 4** Evolution of monomer conversion along the axial direction of the extruder and comparison with experimental results.

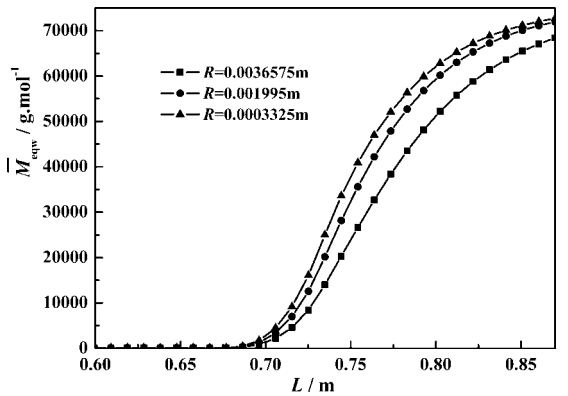


**Figure 5** Evolution of weight-average molecular weight of the fluid along the axial direction of the extruder.

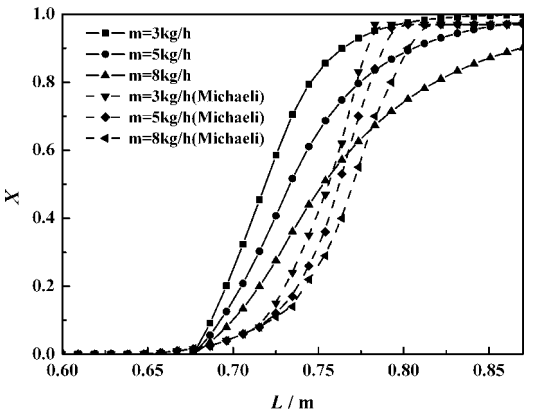


**Figure 7** Influence of flow rate on monomer conversion.

ular weight of the fluid is so small that it can be neglected, and the first item is the increasing function of the monomer conversion, so the weight-average molecular weight of the fluid increases along the axial direction of screws; and (3) both $c$ and $\overline{M}_w$ in eq. (9) are the increasing function of the monomer conversion, and so the zero shear viscosity is the increasing function of the conversion; but at the same time the zero shear viscosity is the decreasing function of the temperature; because the variation range of the temperature in polymerization zone is so small (see Fig. 3) that its influence on the zero shear viscosity is less than those of $c$ and $\overline{M}_w$, and the apparent viscosity is the increasing function of the zero shear viscosity, therefore the apparent viscosity increases along the axial direction of screws.

On the nodes with the same axial length of screws and the different radial distance, the values of variables are different, for the following reasons. In this work, the comprehensive effects of the rotary screws and the static barrel on the fluid flow are equivalent to the effect of the axial motion of the model wall on the fluid flow, so the velocity of the fluid near the wall is bigger than the velocity in the inner, therefore with the increase of the distance to the center line, the residence time of the fluid decreases, and then the monomer conversion, the weight-average molecular weight and the apparent viscosity of the fluid decrease.

The monomer conversion between our simulated results and Michaeli's simulated results as well as experimental result are compared in Figure 4.[4] It can be seen that at the end of the extruder, Michaeli's experimental result is in good agreement with his simulated results, and lies in the center of our three simulated results; the evolution trends of the two types of simulated results are uniform, but in the middle of the screw, our simulated results are bigger than Michaeli's simulated results. The reason is that, compared with the reactor model used in the present study, the ''cascade of continuous stirred tank reactors (CSTRs)'' was adopted by Michaeli. With the model of cascade of CSTRs, the reacting melt passes the individual ideally stirred tanks one after the other, in which there are constant concentrations and temperatures. But in real processes and in our simulation, the concentration and temperature change continuously, and so Michaeli's simulated results are less than our simulated results in the middle of the screw.

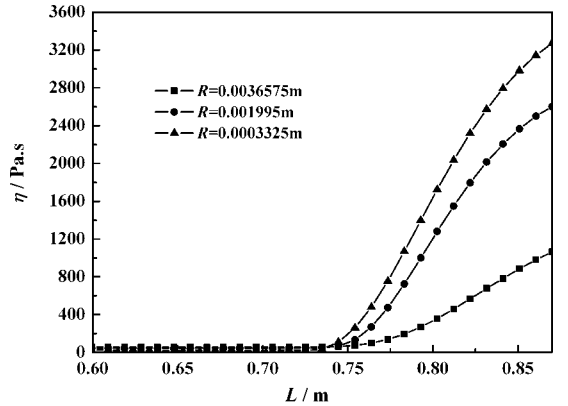


**Figure 6** Evolution of apparent viscosity along the axial direction of the extruder.

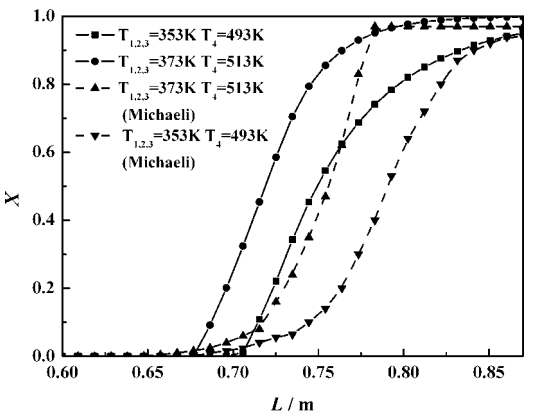


**Figure 8** Influence of temperature on monomer conversion.

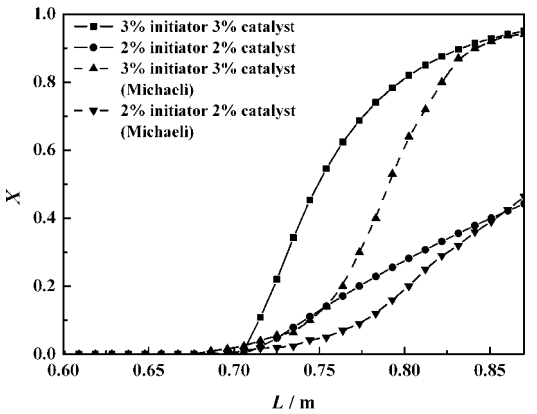


**Figure 9** Influence of initiation system on monomer conversion.

### Influence of processing parameters on reactive extrusion processes

#### Influence of flow rate on monomer conversion

The influence of flow rate on monomer conversion is shown in Figure 7 (The solid lines denote our simulated results, and the dash lines denote Michaeli's simulated results.) It can be seen that with the increase of the throughput, the conversion decreases. The reason is that with the increase of the throughput, the flow rate of fluids increases, and the residence time decreases. Because the conversion is the increasing function of reaction time [eq. (6)], the conversion decreases with the increase of the flow rate.

#### Influence of temperature on monomer conversion

The influence of temperature on monomer conversion can be seen in Figure 8 (The reaction zone was divided into four temperature control pieces,[4] and $T_i$ in Figure 8 represents the temperature of the $i$th piece). With the decrease of temperature, the conversion decreases, because the conversion is the increasing function of temperature [eq. (6)].

#### Influence of initiation system on monomer conversion

The influence of initiator concentration and catalyst concentration on monomer conversion is shown in Figure 9. It can be seen that the conversion decreases with the decrease of initiator concentration and catalyst concentration, and that the monomer conversion is only 44% at the end of the extruder under the condition of low concentrations of initiator and catalyst. This is because the conversion is the increasing function of $A_p$ [eq. (6)], and $A_p$ is the increasing function of the concentrations of initiator and catalyst.[20]

## SUMMARY

The equivalent reactor model and the semi-implicit iterative algorithm have been used to the numerical simulation of the anionic polymerization of PA6 in closely intermeshing co-rotating twin screw extruders, and the evolution of monomer conversion, average molecular weight, and fluid viscosity have been obtained, and the influences of three processing parameters on the reactive extrusion process have been discussed. The simulated results and the experimental result show good correspondence.

Because the construction of the screw reactor model is based on the screw geometry, the model can be extended to large screw diameters.

The twin screw extruder often consists of several elements such as forward conveying screw elements, reverse conveying screw elements, kneading elements and die, and it is not always fully filled actually, so the more precise 3D reactor model should be built. Equation (6) has a better fit to the low monomer conversion phase and, because of the influence of diffusion on reaction rate at the high monomer conversion phase, the polymerization kinetic equation should be more complex and studied. In addition, further experimental results are needed to verify the simulated results.

## References

1. Illing, G. Kunststofftechnik 1968, 7, 351.
2. Illing, G. Mod Plast 1969, 8, 70.
3. Menges, G.; Bartilla, T. Polym Eng Sci 1987, 27, 1216.
4. Michaeli, W.; Grefenstein, A.; Berghaus, U. Polym Eng Sci 1995, 35, 1485.
5. Michaeli, W.; Grefenstein, A. Adv Polym Technol 1995, 14, 263.
6. Berghaus, U.; Bartilla, T.; Heideneyer, P.; Crolla, G. Plastverarbeiter 1988, 39, 86.
7. Hornsby, P. R.; Tung, J. F. J Appl Polym Sci 1994, 54, 899.
8. Kye, H.; White, J. L. Int Polym Proc 1996, 11, 129.
9. Kye, H.; White, J. L. ANTEC Conf Proc 1996, 1, 309.
10. Kye, H.; White, J. L. J Appl Polym Sci 1994, 52, 1249.
11. Kim, B. J.; White, J. L. J Appl Polym Sci 2004, 94, 1007.
12. Geng, X. Twin Screw Extruders and Its Application; China Light Industry Press: Beijing, 2003.
13. Zhu, F. Extrusion Theory and Application; China Light Industry Press: Beijing, 2001.
14. Pan, Z. Polymer Chemistry; Chemical Industry Press: Beijing, 1997.
15. Harry, R. A.; Frederick, W. L.; James, E. M. Contemporary Polymer Chemistry; Science Press: Beijing, 2004.
16. Tao, W. Numerical Heat Transfer; Xi'an Jiaotong University Press: Xi'an, 2001.
17. William, D. R.; Robert, K. P. J Appl Polym Sci 1986, 31, 763.
18. Rubinstein, M.; Colby, R. H. Polymer Physics; Oxford University Press: Oxford, UK, 2003.
19. Wu, Q.; Wu, J. Polymer Rheology; Higher Education Press: Beijing, 2002.
20. Lin D, J.; Ottino, J. M.; Thomas, E. L. Polym Eng Sci 1985, 25, 1155.